Available online at www.sciencedirect.com
SCIENCE DIRECT®
Engineering Fracture Mechanics 72 (2005) 1254–1267
Engineering Fracture Mechanics
www.elsevier.com/locate/engfracmech

Fracture instability and limit strength condition in structures with re-entrant corners

Alberto Carpinteri *, Nicola Pugno

Department of Structural Engineering, Politecnico di Torino, Corso Duca degli Abruzzi 24, 10129 Torino, Italy

Received 12 May 2003; received in revised form 13 May 2004; accepted 10 September 2004
Available online 24 November 2004

Abstract

When considering a structural element with a re-entrant corner, the experimental analysis shows how the fracture strength increases with the angle of the corner. Thus, the strength increases with a decrease of the mass of the structure, in contrast to what we are used to observe in different kind of collapses, e.g., plasticity. To predict this behaviour, a non-local theory, basically based on the Novozhilov's hypothesis of existence of a fracture quantum, is herein presented. Theoretical predictions for the strength of finite structures (e.g., finite plates under tension or beams under bending) by varying both angle and relative depth of the corner are presented: accordingly, simple formulas, useful in the design of such structures, are provided. The theory is then compared with experimental and numerical results, showing a relevant agreement.
© 2004 Elsevier Ltd. All rights reserved.

Keywords: Fracture; Strength; Re-entrant corners; Non-local fracture; Fracture quantum

1. Introduction

Non-local fracture criteria are powerful methods in the study of crack propagation. In [1] Novozhilov presents a non-local tensional criterion based on the existence of a fracture quantum. He identified the fracture quantum with the atomic size of the crystalline lattice. On the other, his criterion is basically a non-local stress criterion, and can treat also materials in which the link to the atomic structures is absent, as shown by the Novozhilov's apprentices and recently emphasized in [2]. We apply this method to study analytically the problem of the strength against fracture of structures containing re-entrant corners.

* Corresponding author. Tel.: +39 11 56 44 850; fax: +39 11 564 4899 (A. Carpinteri); tel.: +39 115644895; fax: +39 115644899 (N. Pugno).
E-mail addresses: alberto.carpinteri@polito.it (A. Carpinteri), nicola.pugno@polito.it (N. Pugno).

0013-7944/$ - see front matter © 2004 Elsevier Ltd. All rights reserved.
doi:10.1016/j.engfracmech.2004.09.008

Nomenclature

σ_{ij}	stress-field
σ	far-field stress
σ_f	stress of failure
σ_u	strength of the material
K_I	stress-intensity factor for the Mode I
K_{IC}	critical stress-intensity factor for the Mode I
r and φ	the polar co-ordinates
α	power of the stress singularity
S_{ij}	function describing the angular profile of the stress-field
f	shape function
g	generalized shape function for $\gamma = \pi$
b	structure width
a	defect length
γ	re-entrant corner angle
l	structure length (of the three-point bending)
t	structure thickness
P	applied load (on the three-point bending specimen)
P_{CR}	critical load
s	brittleness number
d_0	fracture quantum
Superscript *	refers to generalized quantities for re-entrant-corners
Superscript π	refers to generalized quantities evaluated for $\gamma = \pi$

Since the pioneer paper [3] the problem of stress intensification at the vertex of re-entrant corners has not been sufficiently addressed if compared with its considerable practical importance. Shapes and sizes of notches or re-entrant corners in structural components are studied more frequently than shapes and sizes of cracks. In spite of this, fracture mechanics applied to (long) sharp cracks [4,5] has been broadly developed in the last three decades, even if only as a special case of the more general problem of re-entrant corners.

The investigation on stress intensification at the vertex of re-entrant corners carried out at CSIRO Australian Forest Production Laboratory, Division of Building Research is very notable. In [6] the size scale effects in structures with re-entrant corners due to the presence of a stress-singularity were investigated and noted that they occur only when the member sizes are sufficiently large. Consequently, such scale effects may not appear in scaled-down laboratory testing. The work presented in [6] was continued in [7] extending conventional finite element procedures to non-zero angle notch problems. The author considered also the problem of crack initiation at corners of openings in walls and examined the effect of beam size on the sharp crack propagation in concrete [8].

In [9] the determination of realistic measures for the peak local stresses occurring at sharp re-entrant corners in plates under remote transverse loading has been considered. The authors took up the singular character of re-entrant corners and carried out experimental investigation on classical stress concentration. Then, the Reciprocal Work Contour Integral Method was used to obtain the stress singularity at the tip of corner configurations [10]. In this way, the numerical analysis of a lap joint with $\pi/2$ corner angles in mixed mode loading has been performed.

In [11] the expression of the brittleness number to study the transition between brittle and ductile collapses [12–14] and the stress-intensity factor at the vertex of a re-entrant corner applying Buckingham's Theorem has been generalized. In the same paper a shape function for generalized stress-intensity factor, assuming a combination of LEFM and ultimate strength function, is defined. According to the last hypothesis and to the results of an experimental investigation, the values of stress-intensity factors varying the corner angle are reported.

More recently some authors [15] have obtained numerically, by FEM, the shape function for a re-entrant corner with particular angles (0, $\pi/2$, $2\pi/3$). In Ref. [2] a relation between the stress-intensity factor for a corner and that for a crack, obtained from the Novozhilov's brittle fracture criterion [1], is presented. This criterion is based on the hypothesis that the fracture of solids is a discrete process: the destruction of the connection between just one pair of atoms will be a fracture quantum. In [16] the stress and strain fields at the vertex of a corner subjected to different boundary conditions, in plane problems of elasticity, have been studied. In reference [17] the relation presented in [2] for the generalization of the stress-intensity factor is taken into account. In [18] the problem of evaluating linear elastic stress fields in the area of cracks and notches by Muskhelishvili's method based on complex functions has been consider. The stress-intensity factors of angular corners have been also calculated for various geometrical and loading conditions by numerical solutions of singular integral equations [19].

Purpose of the present paper is the prediction of the failure load for a structural member with a re-entrant corner [20,21]. An interesting study on this topic is presented in [22]. By focusing attention on an element of material ahead of the notch, failure by yielding and/or fracture has been predicted from the stationary values of the volume energy density regardless of the order of the notch tip stress singularity. Fracture initiation is associated with the critical value of the volume energy density being characteristic of the material. As the stress singularity increases with decreasing notch angle, the critical applied stress to initiate failure decreases.

The theory presented herein agree with the results obtained by the different approaches presented in [23–25] and with the experimental results of the investigation reported in [11]. In addition, the paper solves an old problem posed several years ago in [11], regarding the shape functions for structures with re-entrant corners. The solution is based on the fracture criterion examined in [1] and on the generalized stress-intensity factor obtained in [2]. Tanks to the last expression it has been possible to obtain analytically the generalized shape function defined in [11] and therefore the stress-intensity factor and strength of the structure.

2. Finite plate under tension

Considering a linear elastic plate with a boundary crack (Fig. 1, with $\gamma = 0$), the symmetrical stress field around the tip of the crack can be written as:

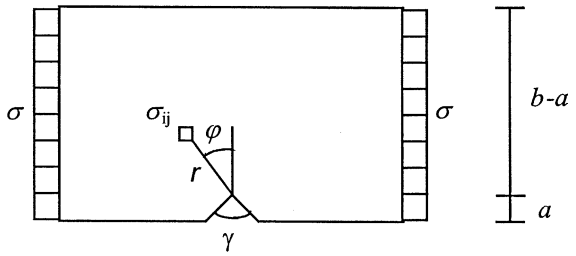

Fig. 1. Finite plate under tension with a re-entrant corner.

$$\sigma_{ij} = K_{\mathrm{I}} r^{-1/2} S_{ij}(\varphi) \tag{1}$$

where K_{I} is the stress-intensity factor for the Mode I, r and φ are the polar co-ordinates represented in Fig. 1 and S_{ij} is a function describing the angular profile of the stress field.

For every structure it is possible to express the stress intensity factor as:

$$K_{\mathrm{I}} = \sigma b^{1/2} f(a/b) \tag{2}$$

where σ is the nominal stress, b is a characteristic size of the structure, a is the crack length and f is a shape function depending on the structural geometry and on the ratio a/b. The stress of failure σ_{f} is achieved when K_{I} is equal to its critical value K_{IC}:

$$K_{\mathrm{IC}} = \sigma_{\mathrm{f}} b^{1/2} f(a/b) \tag{3}$$

The equations presented can be generalized to the case of re-entrant corner with angle γ (Fig. 1).

When both the notch surfaces are free, the symmetrical stress field at the notch tip is [3]:

$$\sigma_{ij} = K_{\mathrm{I}}^{*}(\gamma) r^{-\alpha(\gamma)} S_{ij}^{(\gamma)}(\varphi) \tag{4}$$

where the power α of the stress singularity is provided by the eigen-equation:

$$(1-\alpha)\sin(2\pi-\gamma) = \sin[(1-\alpha)(2\pi-\gamma)] \tag{5}$$

and ranges between 1/2 (when $\gamma = 0$) and zero (when $\gamma = \pi$).

If Buckingham's Theorem for physical similitude and scale modelling is applied and stress and linear size are assumed as fundamental quantities [11] it is possible to write an equation analogous to Eq. (2):

$$K_{\mathrm{I}}^{*}(\gamma) = \sigma b^{\alpha(\gamma)} f^{*}(\gamma, a/b); \quad [K_{\mathrm{I}}^{*}] = [F][L]^{\alpha-2} \tag{6}$$

When the angle γ vanishes, Eq. (6) coincides with Eq. (2), whereas when $\gamma = \pi$ the stress-singularity disappears and the generalized stress intensity factor K_{I}^{*} assumes the physical dimensions of stress and becomes proportional to the nominal stress σ. As experimentally demonstrated in [6], the stress of failure σ_{f} is achieved when the K_{I}^{*} is equal to its critical value K_{IC}^{*}:

$$K_{\mathrm{IC}}^{*}(\gamma) = \sigma_{\mathrm{f}}^{*} b^{\alpha(\gamma)} f^{*}(\gamma, a/b) \tag{7}$$

If the angle is close to zero the corner becomes a crack and Eq. (7) becomes Eq. (3), where f is the following polynomial function ($a/b < 0.6$):

$$f\left(\frac{a}{b}\right) = 2\left(\frac{a}{b}\right)^{1/2} - 0.4\left(\frac{a}{b}\right)^{3/2} + 18.7\left(\frac{a}{b}\right)^{5/2} - 38.5\left(\frac{a}{b}\right)^{7/2} + 53.9\left(\frac{a}{b}\right)^{9/2} \tag{8}$$

In the opposite case of angle close to π, Eq. (7) becomes:

$$K_{\mathrm{IC}}^{*}(\gamma = \pi) = K_{\mathrm{IC}}^{\pi} = \sigma_{\mathrm{u}} = \sigma_{\mathrm{f}}^{\pi} g(a/b) \tag{9}$$

where the function g takes into account the reduction of the resisting cross section:

$$g\left(\frac{a}{b}\right) = \frac{1}{1-a/b} \tag{10}$$

3. Beam under three point bending

A three point bending specimen with a re-entrant corner (Fig. 2) is now considered. The stress-intensity factor can be expressed as (Fig. 2):

$$K_{\mathrm{I}}^{*}(\gamma) = \frac{Pl}{tb^{2-\alpha(\gamma)}} f^{*}(\gamma, a/b) \tag{11}$$

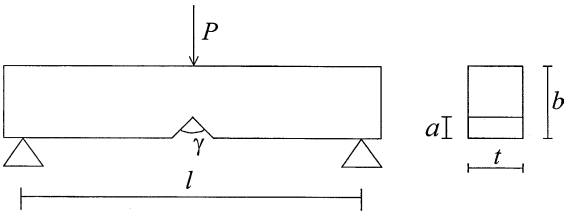

Fig. 2. Three point bending beam with a re-entrant corner.

which, in the critical condition, becomes:

$$K^*_{\mathrm{IC}}(\gamma) = \frac{P^*_{\mathrm{CR}} l}{t b^{2-\alpha(\gamma)}} f^*(\gamma, a/b) \tag{12}$$

where f^* is the unknown generalized shape function. For a crack Eq. (12) assumes the following form:

$$K_{\mathrm{IC}} = K^*_{\mathrm{IC}}(\gamma = 0) = \frac{P_{\mathrm{CR}} l}{t b^{3/2}} f(a/b) \tag{13}$$

where the function f can be expressed as follows ($a/b < 0.6$):

$$f\left(\frac{a}{b}\right) = 2.9\left(\frac{a}{b}\right)^{1/2} - 4.6\left(\frac{a}{b}\right)^{3/2} + 21.8\left(\frac{a}{b}\right)^{5/2} - 37.6\left(\frac{a}{b}\right)^{7/2} + 38.7\left(\frac{a}{b}\right)^{9/2} \tag{14}$$

If the angle becomes flat the generalized stress-intensity factor becomes:

$$K^*_{\mathrm{IC}}(\gamma = \pi) = K^{\pi}_{\mathrm{IC}} = \sigma_{\mathrm{u}} = \frac{P^{\pi}_{\mathrm{CR}} l}{t b^2} g(a/b) \tag{15}$$

where the function g describes the reduction of the resisting cross section:

$$g\left(\frac{a}{b}\right) = \frac{3/2}{(1 - a/b)^2} \tag{16}$$

4. A non-local fracture stress criterion: fracture quantum and generalized stress-intensity factor

In [2] a relation between the stress-intensity factor for a re-entrant corner and that for a crack is obtained from the non-local brittle fracture criterion [1].

The stress field in a cracked plate subject to tension tends to infinity at the crack tip. If it is supposed that the failure occurs when the maximum stress becomes equal to a strength characteristic value, the plate would collapse subject to an infinitesimal external load. In reality, the external load necessary to propagate the crack in the plate is finite, as the energy criterion shows [4]. The paradox between the tensional and the energy approaches can be explained changing the failure criterion assumed above, as done in [1]. This criterion is based on the hypothesis that fracture in solids is a discrete process, i.e., a fracture quantum can be considered. The crack will propagate not when the stress reaches a critical value but when its integral along a quantum of ligament reaches a certain threshold. Accordingly, the brittle fracture criterion [1] should be written in the following integral form:

$$\int_0^{d_0} \sigma_y(x)\,\mathrm{d}x \geqslant \sigma_{\mathrm{u}} d_0 \tag{17}$$

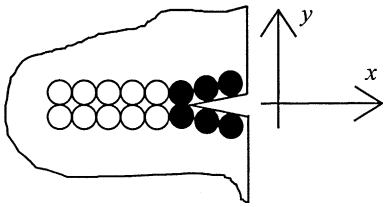

Fig. 3. Discrete fracture propagation in fracture quanta, here represented as spheres.

where σ_u is a strength characteristic value for the material without defects and d_0 is the fracture quantum (Fig. 3). Note that in [1] Novozhilov identified the fracture quantum with the atomic size of the crystalline lattice. However, if this hypothesis is relaxed, a more general non-local criterion is obtained, without any link to the atomic dimension, as shown by the Novozhilov's apprentices and recently reconsidered in [2].

Substituting the stress field around the vertex of the corner (4) into Eq. (17), we can rewrite the condition for brittle propagation as:

$$K_I^*(\gamma) \geqslant [1-\alpha(\gamma)](2\pi d_0)^{\alpha(\gamma)}\sigma_u \tag{18}$$

where the right part of the inequality represents the critical value of the stress-intensity factor:

$$K_{IC}^*(\gamma) = [1-\alpha(\gamma)](2\pi d_0)^{\alpha(\gamma)}\sigma_u \tag{19}$$

Evaluating Eq. (19) for a crack we obtain d_0 (it is interesting to emphasize how the quantum d_0 coincides with Irwin's estimate of the plastic zone diameter):

$$d_0 = \frac{2}{\pi}\frac{K_{IC}^2}{\sigma_u^2} \tag{20}$$

Substituting d_0 into Eq. (19) we can find the relationship presented in [2]:

$$K_{IC}^*(\gamma) = (1-\alpha(\gamma))\sigma_u\left(\frac{2K_{IC}}{\sigma_u}\right)^{2\alpha(\gamma)} \tag{21}$$

5. Generalized brittleness number, shape function and strength

The embrittlement of the structural response produced by the decrease in fracture toughness and/or by the increase in strength σ_u and/or in the size b, can be described in a unitary and synthetic manner via the variation in the following dimensionless number [11,12]:

$$s^*(\gamma) = \frac{K_{IC}^*(\gamma)}{\sigma_u b^{\alpha(\gamma)}} \tag{22}$$

Larger the brittleness number $s^*(\gamma)$, larger the structure ductility. If it is over than a characteristic number $s_0^*(\gamma)$ the ductile collapse ($\sigma = \sigma_u$) precedes the generalized brittle collapse ($K_I^*(\gamma) = K_{IC}^*(\gamma)$) for any relative corner depth a/b. Eq. (22) shows that the brittleness and the ductility are structure-characteristics more than material-characteristics: increasing the size b of the structure its embrittlement increases.

Taking into account Eq. (21), relation (22) may be reformulated in a generalized form:

$$s^*(\gamma) = (1-\alpha(\gamma))(2s)^{2\alpha(\gamma)} \tag{23}$$

In the opposite cases of crack or corner angle close to π (flat angle) we respectively have:

$$s = s^*(\gamma = 0)\frac{K_{IC}}{\sigma_u\sqrt{b}} \tag{24a}$$

$$s^*(\gamma = \pi) = 1 \tag{24b}$$

The last trivial equation has the meaning that for an uncracked structure the generalized brittle and the ductile collapses are coincident.

Considering a three point bending specimen and substituting Eq. (22) into Eq. (12) we obtain the dimensionless failure load as a function of the generalized brittleness number and of the shape function:

$$\frac{P^*_{CR}l}{tb^2\sigma_u} = \frac{s^*(\gamma)}{f^*(\gamma, a/b)} \tag{25}$$

This kind of collapse, when $K^*_I(\gamma) = K^*_{IC}(\gamma)$, is always intermediate between brittle [$K_I = K_{IC}$] and ductile [$\sigma = \sigma_u$] collapses. Eq. (25) can be evaluated for a crack:

$$\frac{P_{CR}l}{tb^2\sigma_u} = \frac{s}{f(a/b)} \tag{26}$$

and for a flat angle:

$$\frac{P^\pi_{CR}l}{tb^2\sigma_u} = \frac{1}{g(a/b)} \tag{27}$$

For a structural element with a crack of a given relative depth, the transition between brittle and ductile collapse [14] arises when the failure loads (26) and (27) are equal, i.e., when:

$$s_0 = \frac{f(a/b)}{g(a/b)} \tag{28}$$

If the angle is different from zero, the crack becomes a re-entrant corner and the transition arises when the failure loads (25) and (27) are equal, i.e., when:

$$s^*_0(\gamma) = \frac{f^*(\gamma, a/b)}{g(a/b)} \tag{29}$$

This competition between the two kinds of collapses (25) and (27) is shown in the diagrams of Fig. 4. The value of the brittleness number for which the corresponding generalized fracture curve (25) is tangential to the curve of ductile collapse (27) represents its characteristic value; for higher values of s^* the ductile collapse precedes the generalized brittle collapse for any relative corner depth.

Substituting Eqs. (28) and (29) into Eq. (23) we obtain the generalized shape function for the re-entrant corner (Fig. 5):

$$f^*(\gamma, a/b) = (1 - \alpha(\gamma))g(a/b)\left(2\frac{f(a/b)}{g(a/b)}\right)^{2\alpha(\gamma)} \tag{30}$$

This interesting result allows, via Eqs. (12) and (21), to obtain the strength for a structure with a re-entrant corner.

The critical stress-intensity factor (for a crack) and the ultimate tensile strength of the material of the element, can be obtained as functions of the failure loads in the cases of angle equal to zero (13) and flat angle (15). Substituting the generalized stress-intensity factor (21) and the shape function (30) into Eq. (12), we can predict the strength for a member with a re-entrant corner:

$$\frac{P^*_{CR}}{P^\pi_{CR}} = \left(\frac{P_{CR}}{P^\pi_{CR}}\right)^{2\alpha(\gamma)} \tag{31}$$

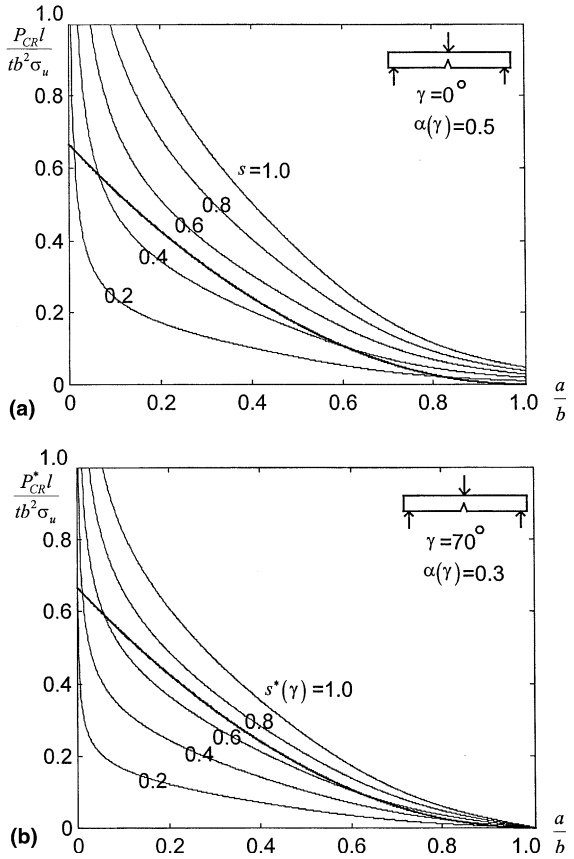

Fig. 4. (a) Competition between brittle (thin lines) and ductile (thick line) collapses, in the case of three point bending beam with edge crack ($\gamma = 0°$). (b) Competition between generalized brittle (thin lines) and ductile (thick line) collapses, in the case of three point bending with re-entrant corner ($\gamma = 70°$).

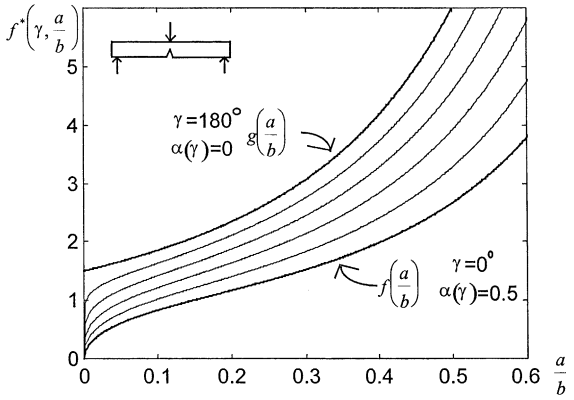

Fig. 5. Generalized shape function for the three point bending beam.

This interesting result allows to predict in a very simple manner the strength of structures with a re-entrant corners. Eqs. (30) and (31) are true also for different schemes such as the finite plate in tension already

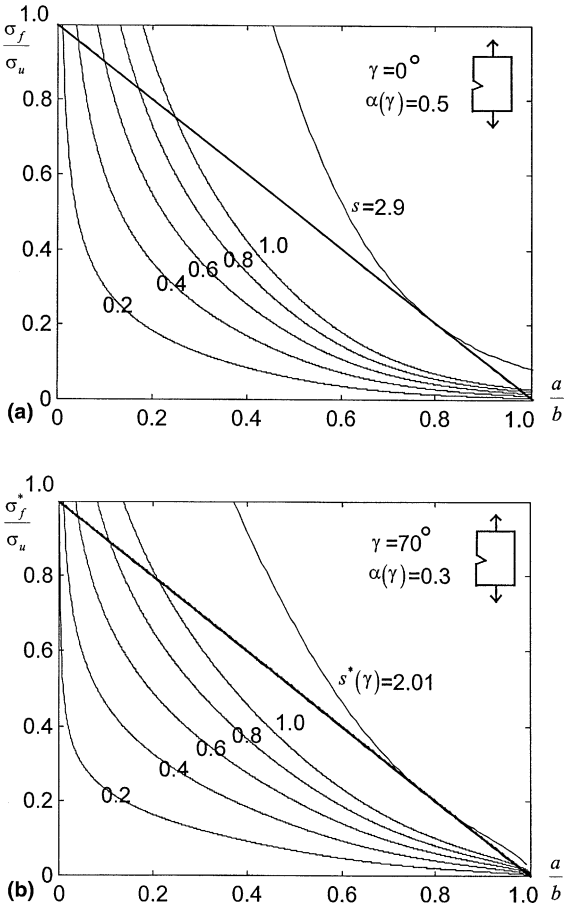

Fig. 6. (a) Competition between brittle (thin lines) and ductile (thick line) collapses, in the case of plate in tension with edge crack ($\gamma = 0°$). (b) Competition between generalized brittle (thin lines) and ductile (thick line) collapses, in the case of plate in tension with re-entrant corner ($\gamma = 70°$).

described, where the failure loads are equal to the failure stresses multiplied by a characteristic area, i.e., $P^*_{CR} \propto \sigma^*_{CR}$. In Figs. 4, 5 the dimensionless strength of a three-point bending beam is reported (on the basis of the shape functions (14) and (16)), whereas in Figs. 6, 7 the plate in tension is considered (shape functions of Eqs. (8) and (10)).

6. Size-effects

Introducing a characteristic maximum value b_{max} of the structure, from the generalized brittleness number (22), we can rewrite Eq. (7) emphasizing the attenuation of the size effects on the failure load when increasing the angle of the corner:

$$\ln \frac{\sigma^*_f}{\sigma_u} = \ln \frac{s^*(b_{max})}{f^*(a/b)} - \alpha(\gamma) \ln \frac{b}{b_{max}} \tag{32}$$

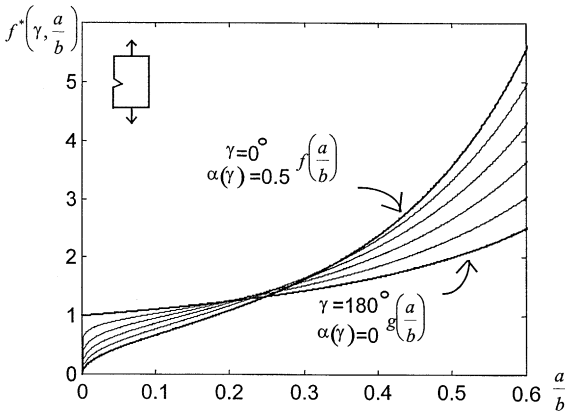

Fig. 7. Generalized shape function for the plate in tension.

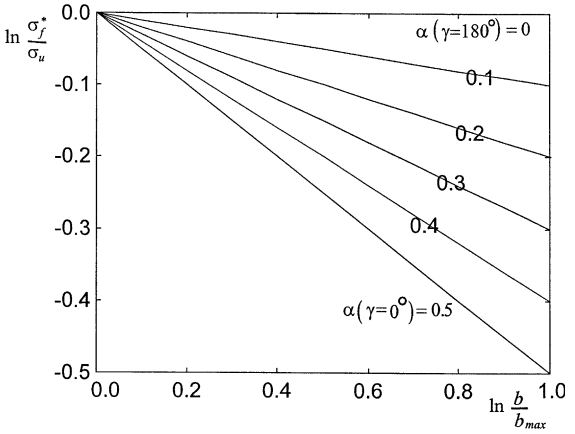

Fig. 8. Attenuation of the size effects increasing the angle of the corner.

If we consider self-similar structures, a/b = constant and as a consequence $\ln \sigma_f^*$ is proportional to $-\alpha \ln b$. In other words, for $\alpha \neq 0$, the failure load decreases with size b. For structure ($\alpha = 0$) without (or with a flat) re-entrant corner the size effects vanish (Fig. 8).

7. Simplified results

Eqs. (21), (23) and (30) allow to obtain the generalized stress-intensity factor, the brittleness number and the shape function for a structure with a re-entrant corner. All these generalized quantities G^* can be written in a unitary manner with reference to their known values for an angle equal to zero, G, or for a flat angle, G^π:

$$\frac{G^*(\gamma)}{G^\pi} = 2^{2\alpha(\gamma)}(1-\alpha(\gamma))\left(\frac{G}{G^\pi}\right)^{2\alpha(\gamma)} = \beta(\alpha(\gamma))\left(\frac{G}{G^\pi}\right)^{2\alpha(\gamma)} \tag{33}$$

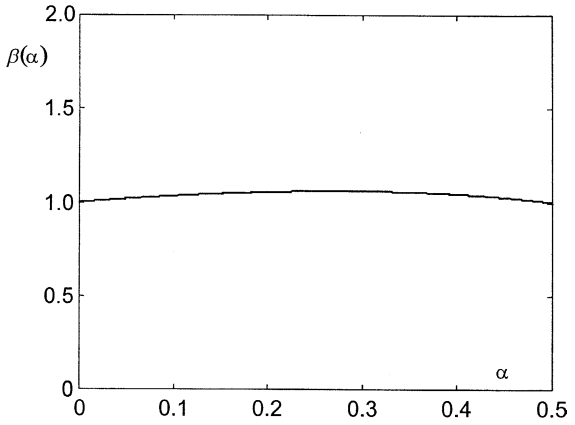

Fig. 9. Quasi-unitary value of the β coefficient.

where coefficient β is approximately constant and equal to one, as Fig. 9 shows. Its maximum divergence from one is 6%. If we put $\beta = 1$ in Eq. (33) we can obtain the following simplified equation:

$$\frac{G^*(\gamma)}{G^\pi} = \left(\frac{G}{G^\pi}\right)^{2\alpha(\gamma)} \tag{34}$$

This equation allows to describe also the generalized failure load (31) and can be defined as the fundamental equation to generalize any quantity for a re-entrant corner. The theory is applicable to different schemes and also with re-entrant corners not subjected only to Mode I; actually the approach proposed in Section 4 remains valid for crack propagation Mode II or III, considering the corresponding stress-intensity factors and the shearing stresses instead of the normal ones.

8. Experimental and numerical assessments

The theory presented has been validated experimentally. Three point bending specimens of PMMA with two different relative depths of the re-entrant corner ($a = 1.2$ cm, $b = 5$ cm, $t = 5$ cm, $l = 19$ cm) and six different angles, for a total of twelve specimens, have been tested. The results of their failure loads are reported in [11]. From Eq. (31) we can obtain the corresponding theoretical predictions. The comparison between theoretical and experimental results is shown in Fig. 10 by varying both the angle and relative depth of the re-entrant corner. The results show basically a relevant agreement between the theoretical and the experimental approaches.

In addition to the previous experimental assessment, a comparison with the numerical results on re-entrant corners reported in [23–25] and [26] is considered. In [25] the predictions reported in [23,24] were compared, demonstrating their equivalence. A good correspondence between the results in [24] and in [26] is emphasized in [24]. Thus, references [23–25] and [26] are equivalent to make a comparison. We consider the numerical FEM results reported in [24]. The analysed case is a finite plate under tension containing a re-entrant corner. From Eqs. (6), (8), (10) and (30) we can analytically predict the values of the stress-intensity factors K_I^*. Note that, according to our approach and to the definition for the stress-intensity factor $K_I^*(\text{num})$ given in [24], we have to compare $K_I^*(\text{num})$ with $K_I^*(\text{theo}) = k(\gamma)K_I^*$, where $k(\gamma) = \frac{1}{2}(2 - \alpha - (1-\alpha)\cos(\gamma) - \cos[(2\pi - \gamma)(1-\alpha)])$, satisfying $k(\gamma = 0) = 1$. The comparison between theory and numerical solutions is reported in Tables 1 and 2, by varying respectively the angle and the relative

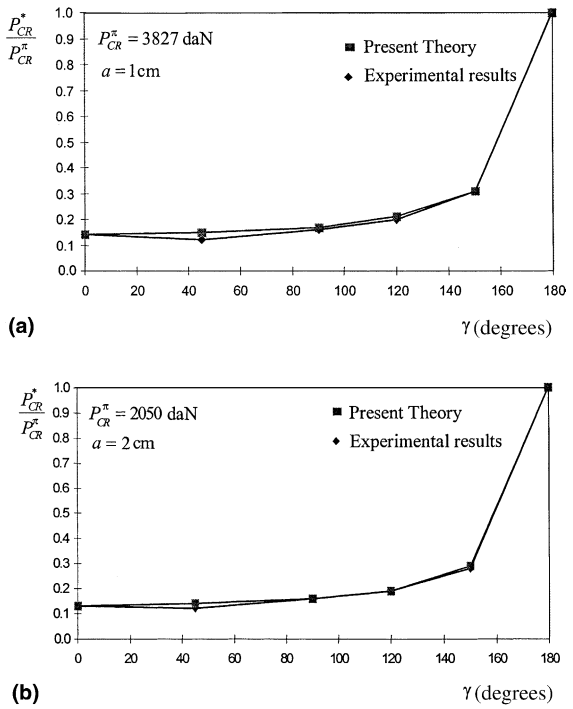

Fig. 10. (a) Experimental-theoretical comparison for the strengths of a three point bending specimen with corner of relative depth 0.2. (b) Experimental and theoretical comparison for the strengths of a three point bending specimen with corner of relative depth 0.4.

Table 1
Numerical-theoretical comparison for the generalized stress-intensity factor by varying the angle of the corner (relative depth equal to 0.4)

Angle (degree)	$\frac{K^*_I(\text{num})}{\sigma\sqrt{\pi}a^{\alpha}}$	$\frac{K^*_I(\text{theo})}{\sigma\sqrt{\pi}a^{\alpha}}$
0	2.10	2.11
10	2.11	2.12
30	2.12	2.15
60	2.23	2.25
90	2.46	2.40

Table 2
Numerical-theoretical comparison for the generalized stress-intensity factor by varying the relative depth of the corner (corner angle equal to 90°)

Relative depth	$\frac{K^*_I(\text{num})}{\sigma\sqrt{\pi}a^{\alpha}}$	$\frac{K^*_I(\text{theo})}{\sigma\sqrt{\pi}a^{\alpha}}$
0.2	1.60	1.59
0.3	1.94	1.91
0.4	2.46	2.40
0.5	3.32	3.19
0.6	4.79	4.49

depth of the corner. Also in this case a good agreement is found. Note that the comparison does not involve a best-fit parameter.

Additional results on re-entrant corners in similar but different contexts can be found in [27], where strips are analysed, and in [28], the Murakami's handbook, where the problem of a crack originating from a re-entrant corner in a semi-infinite plate under bending is reported.

9. Conclusions

In this paper we have proposed an analytical solution for the problem of the prediction of the strength for structures containing re-entrant corners. It is based on a non-local stress failure criterion. Even if the theoretical approach is not trivial, the final result, i.e., Eq. (31), is very simple and can be easily applied in the design of mechanical and civil components. A simplified equation, i.e., Eq. (34), is finally proposed to generalize for a given corner angle its main quantities such as strength, stress-intensity factor, shape function, brittleness number and fracture toughness or material strength, starting from their well-known values for flat angle (describing a cross-section reduction) and for vanishing angle (describing a crack). The method is sufficiently general and can be applied to different schemes and failure modes. Finally, we have shown that our approach agrees with experimental and numerical analyses by varying both angle and relative depth of the corner.

Acknowledgments

The present research was carried out with the financial support of the Ministry of University and Scientific Research (MURST), the National Research Council (CNR) and the EC-TMR Contract N°ERBFMRXCT960062.

References

[1] Novozhilov V. On a necessary and sufficient criterion for brittle strength. Prik Mat Mek 1969;33:212–22.
[2] Seweryn A. Brittle fracture criterion for structures with sharp notches. Engng Fract Mech 1994;47:673–81.
[3] Williams ML. Stress singularities resulting from various boundary conditions in angular corners of plates in extension. J Appl Mech 1952;19:526–8.
[4] Griffith AA. The phenomenon of rupture and flow in solids. Phil Trans Roy Soc 1921;28:163–98.
[5] Irwin GR. Analysis of stresses and strains near the end of a crack traversing a plate. J Appl Mech 1957;24:361–4.
[6] Leicester RH. Effect of size on the strength of structures, CSIRO Division of Building Research 1973, Paper No. 71.
[7] Walsh PF. Linear fracture mechanics solutions for zero and right angle notches. CSIRO Division of Building Research 1974, Paper No. 2.
[8] Walsh PF. Crack initiation in plain concrete. Mag Concrete Res 1976;28:37–41.
[9] Sinclair GB, Kondo M. On the stress concentration at sharp re-entrant corners in plates. Int J Mech Sci 1984;26:477–87.
[10] Carpenter WC. Mode I and Mode II stress intensities for plates with cracks of finite opening. Int J Fract 1984;26:201–14.
[11] Carpinteri A. Stress-singularity and generalized fracture toughness at the vertex of re-entrant corners. Engng Fract Mech 1987;26:143–55.
[12] Carpinteri A. Notch sensitivity in fracture testing of aggregative materials. Engng Fract Mech 1982;16:467–81.
[13] Carpinteri A. Plastic flow collapse versus separation collapse in elastic–plastic strain-hardening structures. Mater Struc 1983;16:85–96.
[14] Carpinteri A, Marega C, Savadori A. Ductile–brittle transition by varying structural size. Engng Fract Mech 1985;21:263–71.
[15] Dunn ML, Suwito W, Cunningham S. Fracture Initiation at sharp notches: correlation using critical stress intensities. Int J Solids Struct 1997;34:3873–83.
[16] Seweryn A, Molsky K. Elastic stress singularities and corresponding generalized stress intensity factors for angular corners under various boundary conditions. Engng Fract Mech 1996;55:529–56.

[17] Grenestedt JL, Hallstrom S, Kuttenkeuler J. On cracks emanating from wedges in expanded PVC foam. Engng Fract Mech 1996;54:445–56.
[18] Lazzarin P, Tovo R. A unified approach to the evaluation of linear elastic stress fields in the neighborhood of cracks and notches. Int J Fract 1996;78:3–19.
[19] Noda NA, Oda K, Inoue T. Analysis of newly-defined stress intensity factors for angular corners using singular integral equations of the body force method. Int J Fract 1996;76:243–61.
[20] Carpinteri A, Pugno N. Intensificazione degli sforzi, funzione di forma e numero di fragilità per elementi strutturali provvisti di angoli rientranti. In: Proc. XIV Italian Conf Theor Appl Mech, 6–9 October 1999, Como, Italy, CD-ROM N, 214.
[21] Carpinteri A, Pugno N. Structural elements with re-entrant corners. In: Proc XV Italian Conf Fract (IGF), 391–98, 3–5 May 2000, Bari, Italy.
[22] Sih GC, Ho JW. Sharp notch fracture strength characterized by critical energy density. Theor Appl Fract Mech 1991;18:179–214.
[23] Gross B, Mendelson M. Int J Fract Mech 1972;8:267–76.
[24] Lin KY, Ping Tong. Singular finite elements for the fracture analysis of V-notched plate. Int J Num Methods Engng 1980;15:1343–54.
[25] Chen DH. Int J Fract Mech 1995;8:81–97.
[26] Gross B. Some plane problems elastostatic solution for plates having a V-notch. PhD Thesis, Case Western Reserve University (1970).
[27] Chen DH. In: Proc 11th Int Conf Exp Mech, Oxford UK, 1998:1161–6.
[28] Murakami Y. Stress intensity factor handbook. Pergamon Press; 1987.